Simplifying Through-Forest Propagation Modelling

ROSHANAK ZABIHI (Student Member, IEEE), AND RODNEY G. VAUGHAN, (Life Fellow, IEEE)

Sierra Wireless Communication Lab, Engineering Science Department, Simon Fraser University, Burnaby, BC V5A 1S6, Canada

CORRESPONDING AUTHOR: R. ZABIHI (e-mail: rzabihi@sfu.ca)

ABSTRACT Propagation analysis and modeling is critical for radio systems design, but remains a challenge for most through-vegetation situations, including forests. Transmission through such inhomogeneous mixed media is complicated by the many different propagation mechanisms and the complexity of the randomness. This means that accurate, purely physics-based analysis is unlikely to be practical (conveniently computed), and similarly, that practical, purely random modeling is unlikely to be accurate. Through-vegetation propagation models, including the standard radiative energy transfer (RET), are not very accurate in the sense that the uncertainty can be tens of dB, and this seems to be an accepted limitation for vegetation. A simpler propagation model, which maintains or improves accuracy, but keeps a reasonable association with the physics, would be insightful. This paper discusses such a model. It comprises two parallel transmission mechanisms: direct transmission through a succession of trees, which is modeled by a simple linear transmission line; and transmission across the forest top, which is modeled by simplified multiple-edge diffraction. The model is examined using recently-published experiments over a long path-length. It is demonstrated that this two-mechanism model can provide an accurate fit to the dual-slope profile of through-forest propagation over a long distance which is not possible with the RET model.

INDEX TERMS Propagation modeling for vegetation, multi-layered transmission line, multiple-edge diffraction.

I. INTRODUCTION AND BACKGROUND

RADIO communications has become a major part of our lives, with wireless being the primary access to the Internet. Almost all terrestrial radio communication links are non-line-of-sight (NLOS) with the multipath dispersion creating distortion in the communications signals. Fixing the distortion has driven the development of sophisticated communications techniques and led to a significant legacy of signal theory and signal processing. This legacy is now part of the backbone of modern estimation and array techniques, and in fact is still experiencing rapid development, still driven by demand for ever-increasing wireless services. For sensing, radar is traditionally LOS, although applications have extended to NLOS systems such as through-the-wall imaging, landmine detection, and through-cover scenarios such as airport personal screening. There is also interest in terrestrial radar through vegetation in order to detect metallic bodies or some other unusual reflection through dense foliage.

For all these applications, analysis of the radio channel is critical for configuring the link, including the antennas.

Progress in propagation modeling, in particular through vegetation, has not kept pace with wireless deployment. Current propagation models for the various scenarios, are inaccurate in the sense that several (up to tens) of dB of uncertainty is common. However, much progress has been made on the electromagnetic analysis of canonical situations, such as the diffraction of idealized single [1]–[3] and multiple edges [4]–[10]. A single mechanism, even a critical one such as diffraction, seldom dominates all the coverage zones of a real-world link. Very few experiments have been reported on diffraction [11]–[13]. Similarly, there are few measurements of propagation through vegetation, mostly with very high uncertainty, and yet these are the basis of standard models (see below). Ray tracing is a popular technique for multipath propagation modelling, but is best suited for a smooth-surface geometric model, such for a city where the building geometry is either already publicly available or can be readily derived from public databases or map resources [14]. Reflections and diffractions are used, although there is no standard for how many rays (and how many

reflections and diffractions), and/or what minimum path gain, etc., is used as a criteria to terminate the ray-tracing process.

The physics of radiowave propagation through vegetation is extremely complicated. The mechanisms include: penetration (a direct wave permeating the dielectric vegetation obstacles); multiple scattering between the wide variety of vegetation components; reflection off the ground, or even a surface wave along the ground; rough surface reflection and scattering; diffraction around and over the vegetation obstacles; and forward scattering along the outside boundaries of the vegetation. (It is assumed here that the propagation around a forest is negligible, which seems reasonable for point-to-point deep within large forest.) These mechanisms are all extremely difficult, if not impossible, to model accurately for a real-world situation. The analysis of propagation through/around even a single tree is fraught, and as noted above, physical measurements still form the basis of models, which still have high uncertainty. The analysis for propagation through extended vegetation, such as just a few trees, or a forest, is similarly fraught, and again the parameters for standard models (such as RET, specified for short distances only) are empirical.

A standard approach to scattering loss is to characterize the media as containing randomly spaced discrete scatterers from a statistical overlay. In such an approach, the dominant mechanism causing excess propagation loss is the scattering of the energy away from the point-to-point path [8], [15]. Empirical models based on measurement results can be included as parameters of such a model. The empirical models of [16]–[22] are widely used against specific measurements results. Recent measurements are mainly for the so-called 5G bands, which are higher frequencies than the 1GHz measurements [23] of interest for this paper. 5G frequencies have a much lower range because of the decreased path gain of the higher frequencies. For example, [24] reports 28GHz measurements for distances up to 300m, and the reader is also referred to the references therein for samples of recent papers featuring higher frequency measurements and model-fitting.

There are analytical models [25] which can be based on physics models for canonical (statistical) situations. One approach is based on classical wave theory and uses a fractal-based scattering overlay, and is reported to work well for "large" propagation distances [26]–[28] (meaning in this case up to 500m, whereas below we consider large to mean well over 2000m). An earlier, prominent theory is the diffusion process-oriented RET, also called Transport Theory [29], [30]. This theory models propagation through a statistically homogeneous (so the randomness is "simple") continuum of electrically small absorbing scatterers in free space. The excess loss mechanisms of the RET are the scattering away from the point-to-point direction and the absorption by the scatterers. No other mechanisms are included, such as diffraction around a body. RET is equivalent to Boltzmann diffusion, is mathematically complicated, and it contains a relatively large number of parameters [29], [30].

In the absence of other classical models (alternative works, such as [26]–[28] are more recent), the RET model has been assumed as suitable for embedded-in-foliage scenarios [29]–[31], and was adapted for through-vegetation propagation laid out in ITU-Rec.833-9 [18]. The scenarios even include a single-tree obstacle - which is a major departure from its founding physics. In the ITU-Rec.833-9, the complicated parameters of the complicated RET formulation are empirically set based on very few measurements which usually have few, or even single, observations (i.e., not a respectable statistical ensemble). The end product is a complicated empirical model which maintains the high uncertainty of the empirical parameters used for the curve fitting. For species other than those in existing measurements, or for other radio frequencies and other foliage characteristics, interpolation and extrapolation from the existing experimental data is used to determine the parameters [31].

Despite the empirical approach, the RET-based model does not tend to give very accurate loss prediction even for the specific conditions corresponding to the measurement data. (It is emphasized that "accurate" in statistical propagation modeling and prediction, can still mean an uncertainty of some 10dB, or even several tens of dB). To improve the RET model, larger and statistically-planned physical measurement campaigns are required, but new and improved data cannot reduce its complexity. Therefore, there is interest in a simpler propagation model for through-vegetation, that can be empirical and should yield results which are at least as good as the RET model. Published physical experiments are surprisingly sparse (and more would be extremely welcome), but they seem to indicate, in an ensemble sense, reasonably simple mean path gain behaviour.

This paper discusses a through-forest model which strives to maintain some of the physics by looking at just two mechanisms: penetrative transmission directly through the randomly-layered media of a forest (similar to RET in this sense, although no explicit connection is required to the physics of electrically small scatterers), and along the free-space dominated forest top. Although the equations are known for these propagation mechanisms, a review of them is included below for completeness of this paper. Applications include terrestrial point-to-point links, for fixed links such as cellular backhaul, where trees seem to get in the way surprisingly often, but in particular for long-distance through-forest communications, such as an Internet-of-Things system requiring device-to-device communications between small terminals and a cellular type network or other mobile communications links such as cellphones, within a forest. The new contributions here include the use of the very simple transmission line model for short-distance (up to about 200m) behaviour with a very simple diffraction-derived model for long-distance (over 500m) behaviour, and their linear combination for both the dual-slope behaviour and the

transition between the slopes to match to experimental data. These experiments are recent [23], describing propagation over a long distance through a forest, using a narrow-band system to achieve the large dynamic range. The RET model can also produce a dual slope phenomena, but its parameters cannot be configured to accurately follow the dual slope behaviour of the long distances of the measurements of [23]. (See Table 2 below.)

II. PROPAGATION MODEL
A. PATH GAIN BASICS
The Friis transmission equation gives the context for defining the path gain [8],

$$\frac{P_r}{P_t} = G_t.G_r.G_{path}.\eta \qquad (1)$$

where P_r and P_t are the usual received and transmitted powers, respectively, G_t and G_r are the transmit and receive antenna effective gains which must be well-defined, and the various efficiency factors (in particular the polarization efficiency) are collected in η. In multipath, these factors are taken as statistically independent, and they combine within (1) which defines the path gain, G_{path}.

For the special case of free space media, the path gain corresponds to the spherical spreading. For the Friis approach, the path gain has an inverse frequency dependence stemming from considering an electrically-dimensioned (in square wavelengths) receiving aperture, which is spaced by distance d meters between the phase centers of the antennas, $G_{path} = G_{path}^{(FS)} = (4\pi d/\lambda_0)^{-2}$. (This frequency dependence is normally omitted in acoustics and optics formulations.)

In multipath media which couples the polarizations randomly, the (mean) polarization efficiency becomes a half, and relatedly, for any single port antenna in full-sphere, homogeneous, uncorrelated multipath, the (mean) antenna gain reduces to half of its radiation efficiency [8]. In this way, for propagation through vegetation, the antenna gain depends on the illuminating wave scenario, and this alone can introduce several tens of dB of variation (as a constant offset value) in the path gain estimate. This variation is from choosing an antenna gain to be the radiation efficiency over two at one extreme (the dense multipath likely in a dense forest), and the usual maximum co-polarized directional gain at the other extreme (free space), or something in between depending on the multipath model and the pattern of the antenna.

With definitions for the antenna gains in place (and associated offsets in the path gain estimate), the measured received power gives the path gain through vegetation. It can be extremely variable for a given transmit-receive distance. A single narrow-band measurement is subject to the Rayleigh-like fading, with a variation at least 30dB. Averaging over the Rayleigh-like fading gives an estimate of the local mean path gain, although good accuracy of the mean estimate requires a large number of local spatial measurements (or spaced apart in frequency using a wideband measurement) [8].

Different experimental approaches treat these offset-producing factors differently (if at all), so the slopes of the path gain with distance become the more interesting feature for analysis and modeling. The local variations in the mean estimate are then considered to be the numerous propagation media factors: foliage densities and sizes, species, seasons, and of course, different propagation frequencies [32].

It has been observed experimentally [29], [30] that a signal is strongly attenuated at short distances due to absorption and scattering by leaves and branches, while at larger distances (in this context meaning about 100m), in-line scattering becomes a dominant mechanism of propagation resulting in a lower attenuation rate. This foliage path loss is also been referred to as a dual-slope propagation loss, e.g., [28] on a log-linear scale. These experimental observations suggest that a simpler model than the RET approach, comprising just two propagation mechanisms, should be feasible. For example, separate transmission line models have been discussed in the context of dual slope path gain using the variables as the pair of slopes and the breakpoint separating them, for a given frequency [33].

The long distance (up to 2580m) experiments also show a dual slope in log-log scale [23]. The slope of the short-distance transmission can be somewhat less than free space, and [23] fits this with a two-ray model in free space. The RET model (not considered in [23]) can also fit to such behaviour. Here we take a compromise by using a transmission line model for the short-distance. This is much simpler than the RET model, and may be closer to the physics of the dense scattering of a forest than the pair of free-space rays used in [23]. In our (linear) transmission line model [34], [35], the wave is guided linearly, and so the attenuation mechanism is, instead of spherical spreading and rescattering, only from passing through the lossy sections of the line. These transmission line sections can be spaced akin to an effective tree spacing. The lossy sections of the linear transmission line are here very low loss (all transmission line sections have a free space real permittivity, and the tree sections have a small loss added, see below), and so the reflections in the transmission line are negligible. In this way, we do not need the extra complexity of cylindrical or spherical transmission lines. A limitation of this model is that physically reflected power may not be well modelled. It is reasonable to attribute the long-distance propagation to diffraction over the top of the trees. For this we can use multiple knife-edge diffraction [4]–[6]. The output (receive power) is a weighted sum of these two mechanisms (see Fig. 1). The weighting coefficients, $W_1 < 1$ and $W_2 = 1 - W_1$, must be empirical. This model has a minimum of parameters, and retains a reasonable attachment to the physics.

The two propagation mechanisms are treated as independent, so that the diffraction path is not continually fed by the scattering through the trees. This is unlikely to be the case in practice, which is a limitation of our
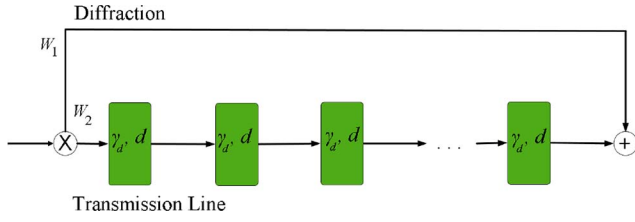
FIGURE 1. Through-forest propagation model. The transmission line, in parallel and uncoupled with the diffraction path.

model, but the independence keeps the model as simple as possible. Time domain measurement (requiring wide bandwidth, which means that the required large dynamic range of the measurement system must have some narrow bandwidth-resolving capability such as OFDM) may resolve this issue, but no long-range wideband measurements are publicly available as far as the authors are aware.

Although the two propagation mechanisms are considered independent (e.g., the transmission line lossy sections do not continually feed the diffraction links), there is a form of dependence between the models of the two propagation mechanisms - the number of transmission line sections is taken as the same as the number of diffraction edges. While this is not strictly necessary for the dual-mechanism model to work, each transmission line section can be viewed as relating a tree with a transmission loss to the same tree having an edge diffraction. So the more transmission line sections, the more diffraction edges. This tends to change the offsets of the various contributions (as do the many other factors, discussed above) but it is the slopes that are of particular interest.

B. MULTI-LAYER TRANSMISSION LINE

The transmit antenna is typically placed away from the trees so the illumination is essentially a plane wave, as illustrated in Fig. 2a. Intuitively, a tree can be modeled as a two-dimensional block, e.g., [33]. For simplicity, the trees are modeled as regularly spaced and with constant thickness, see Fig. 2b. Randomness in the spacing and thickness provides only a second-order effect. The transmission line can be configured in many ways by interchanging between the spacing, thickness and loss of each section (tree), but a choice of fixing both the spacing and the thickness allows fewer parameters and of course simplicity.

The transmission line relations [34], [35] are now briefly summarized for the vegetation modeling. The vegetation has a complex (i.e., lossy) propagation constant for each tree section

$$\gamma_d = j\omega\sqrt{\mu\epsilon} \qquad (2)$$

where $\mu = \mu_0\mu_d$ and $\epsilon = \epsilon_0\epsilon_d$ are respectively the permeability and the permittivity of the dielectric (tree). The relative permeability is $\mu_d = 1$ and the complex relative permittivity is $\epsilon_d = \epsilon'_d - j\epsilon''_d$. μ_0 and ϵ_0 are for free space, and ω is angular frequency. The characteristic impedance of the dielectric is $\eta_d = j\mu\omega/\gamma_d$. The constant thickness of the

(a)

(b)
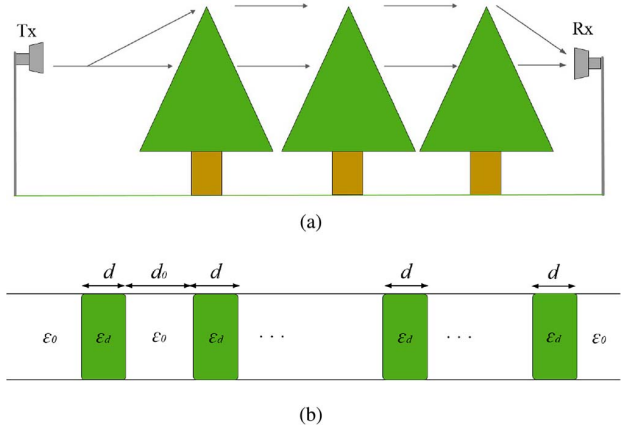
FIGURE 2. (a) A depiction of trees between a transmitter and receiver antenna. (b) Two-dimensional multi-layer configuration of in-line trees. The constant thickness of the trees and the free space distance between them are donated by d and d_0, respectively. The diffraction and vegetation penetration mechanisms are considered as independent, a simplifying limitation, but their models are connected, again for simplicity, by the number of lossy transmission line sections (trees) being the same as the number of diffraction edges (tree tops).
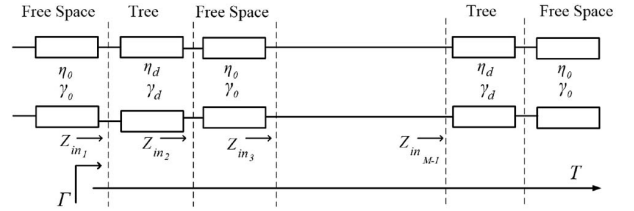
FIGURE 3. Equivalent transmission line circuit for the two-dimensional multi-layered configuration of in-line trees (after [34]).

trees and the free space distance between them are denoted by d and d_0, respectively. The transmission line model for such in-line trees is illustrated in Fig. 3. For the nature and goal of this transmission line model, we do not attempt to differentiate detail such as trunks and leaves, or foliage density for a tree, whereas some curve fitting approaches rely on the trunk size, for example.

The transmission coefficient is

$$T = \left(\frac{2\eta_d}{\eta_d + \eta_0}\frac{2\eta_0}{\eta_d + \eta_0}\cdots\frac{2\eta_0}{\eta_d + \eta_0}\right)$$
$$\times D^{-1}e^{-\gamma_d d - \gamma_0 d_0 - \cdots - \gamma_{-d}d}, \qquad (3)$$

where

$$D = \left[1 - \left(\frac{\eta_0 - \eta_d}{\eta_0 + \eta_d}\right)\left(\frac{Z_{in_2} - \eta_d}{Z_{in_2} + \eta_d}\right)e^{-2\gamma_d d}\right]$$
$$\times \left[1 - \left(\frac{\eta_d - \eta_0}{\eta_d + \eta_0}\right)\left(\frac{Z_{in_3} - \eta_0}{Z_{in_3} + \eta_0}\right)e^{-2\gamma_0 d_0}\right]\cdots$$
$$\times \left[1 - \left(\frac{\eta_0 - \eta_d}{\eta_0 + \eta_d}\right)\left(\frac{\eta_0 - \eta_d}{\eta_0 + \eta_d}\right)e^{-2\gamma_d d}\right], \qquad (4)$$

and the input impedance of the mth layer is, using the lengths of the free-space and tree thickness (see Fig. 3),

$$Z_{in_m} = \eta_d\frac{Z_{in_{m+1}} + \eta_m tanh\gamma_m d_m}{\eta_m + Z_{in_{m+1}}tanh\gamma_m d_m}, \qquad (5)$$
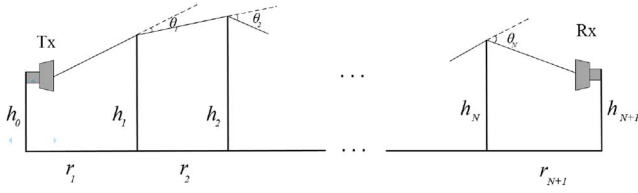
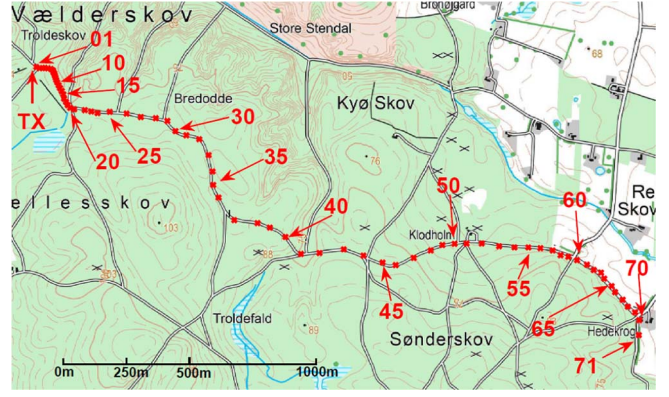**FIGURE 4.** Geometry for multiple knife-edge diffraction (after [6]).

FIGURE 5. Measurement locations conducted in a typical forest terrain in Denmark [23]. The transmitter position is marked as Tx at the left top in the figure.

The incident power relates to the incident electric field as

$$P_{inc} = \frac{|E_0|^2}{2\eta_0}, \tag{6}$$

with $\eta_0 = \sqrt{\mu_0/\epsilon_0} = 120\pi \ \Omega$. The electric field can be calculated from the experimental configuration.

Finally, the power transmitted through the M layers is

$$P_{MLTL_{Trans}} = \frac{|E_0|^2 |T|^2}{2\eta_0}. \tag{7}$$

C. MULTIPLE KNIFE-EDGE DIFFRACTION

A generalized formulation for propagation over various configurations of inhomogeneous terrain is given in [36]. This includes a two-dimensional propagation over multiple rounded obstacles in the form of a residue series, and the knife-edge case when the radius of the curvature decreases to zero. This series was transformed into a multiple integral by Vogler [5], [6] for perfectly absorbing edges. This model is used as a reference for comparison of other techniques such as the Uniform Theory of diffraction (UTD) solution for multiple-edge transition zone diffraction [7]–[9]. The multiple-edge diffraction integral is a very useful tool and the key aspects are briefly summarized here.

The geometry associated with the Vogler multiple knife-edge diffraction is depicted in Fig. 4. The height of the edges above some reference plane are h_i, $i = 1, 2, \ldots, N$, and the height of the transmitter and receiver are h_0 and h_{N+1}. The separation distances between knife-edges are r_i, $i = 1, 2, \ldots, N+1$. The diffraction angles are θ_i, $i = 1, 2, \ldots, N$, obtained from the edge heights and the separation distances. Vogler expresses the excess diffraction loss, which is the attenuation of field strength relative to free space [5], [6],

$$A_N = \left(1/2^N\right) C_N e^{\sigma_N} \left(2/\pi^{1/2}\right)^N I_N, \tag{8}$$

where

$$\sigma_N = \beta_1^2 + \cdots + \beta_N^2, \tag{9}$$

(note that σ, α and β are used differently in this subsection, following convention)

$$C_N = \begin{cases} 1, & N = 1 \\ \left[\dfrac{r_2 r_3 \cdots r_N r_T}{(r_1 + r_2)(r_2 + r_3) \cdots (r_N + r_{N+1})}\right]^{1/2} & N \geq 2 \end{cases} \tag{10}$$

and

$$r_T = r_1 + r_2 + \cdots + r_{N+1}. \tag{11}$$

$$I_N = \int_{\beta_1}^{\infty} \cdots \int_{\beta_N}^{\infty} e^{2f - (x_1^2 + \cdots + x_N^2)} dx_1 \cdots dx_N \tag{12}$$

with

$$f = \begin{cases} 0, & N = 1 \\ \sum_{m=1}^{N-1} \alpha_m (x_m - \beta_m)(x_{m+1} - \beta_{m+1}), & N \geq 2 \end{cases} \tag{13}$$

$$\alpha_m = \left[\frac{r_m r_{m+2}}{(r_m + r_{m+1})(r_{m+1} + r_{m+2})}\right]^{1/2}, \\ m = 1, \ldots, N - 1 \tag{14}$$

$$\beta_m = \theta_m \left[\frac{jk(r_m r_{m+2})}{2(r_m + r_{m+1})}\right]^{1/2}, \\ m = 1, \ldots, N \tag{15}$$

To reduce the computation time, the multiple-edge integral in (12) is transformed into the series of terms involving the repeated integral of the error function, which is reported in [6] for up to 10 knife-edges, after which the general accuracy falls away. But we can use a special case (along the equi-spaced and same-height tree tops) which has a simpler, accurate solution. Experiments with statistical perturbations from this arrangement, using the UTD, have been investigated in [37].

III. RESULTS AND DISCUSSION
A. MODEL COMPARISON
In this section, the model is examined against results from an extraordinary (for their distance, accuracy, and dynamic range from using an extremely narrowband) set of through-forest measurements conducted in a typical forest terrain in Denmark at 917.5MHz, recently published [23]. The trees are predominantly fir (pine), oak, and beech. The foliage density changes significantly between summer and winter because of the deciduous trees. The measurements were taken in summer. The forest is reported to be a mix of coniferous and deciduous trees [23]. The transmitter and receiver have the same height of 1.5m with the transmit power 40dBm, and there are 71 distances along the path. The furthest
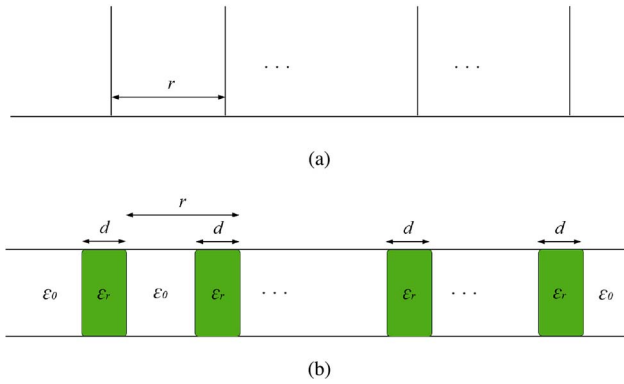
FIGURE 6. (a) *N* absorbing knife-edge diffraction from the crown of the trees with the same height and spacing, *r*, **(b)** Two-dimensional *M*-layer configuration of in-line trees with *d* thickness, ϵ_r dielectric constant and *r* spacing.

measurement position has a straight line distance to the transmitter of 2580m. The forest map and the measurement locations [23] are shown in Fig. 5, and the results of the measurement are included in the figures further below. In these measurements, the short-term, Rayleigh-like fading which is from the vegetation scattering, is averaged at each measurement point, using a circular locus of about 3.3 wavelengths. (In dense multipath, this finite measurement aperture gives a one-standard deviation spread of just over a dB, [8]). In some recent papers, the Rayleigh-like fading is not removed from the propagation measurement at each range point, and it tends to dominate the path gain variations because of its distribution spanning several tens of dB for a narrow-band signal.
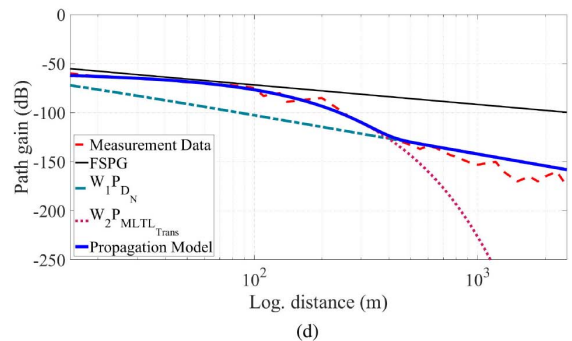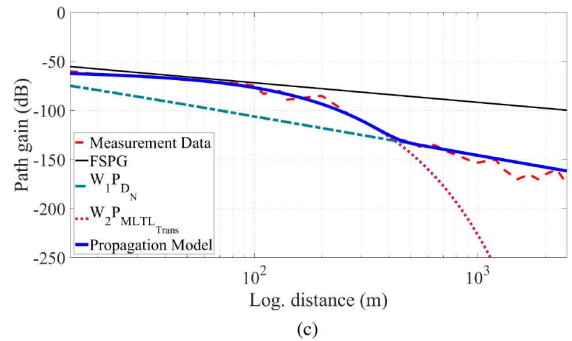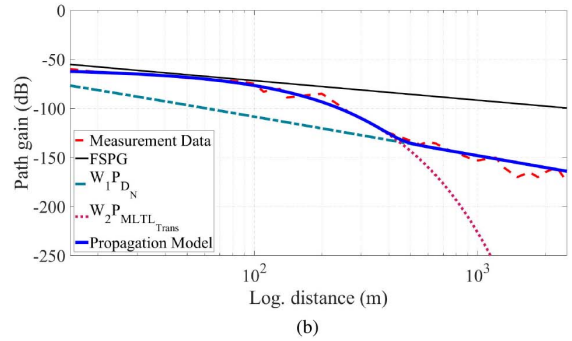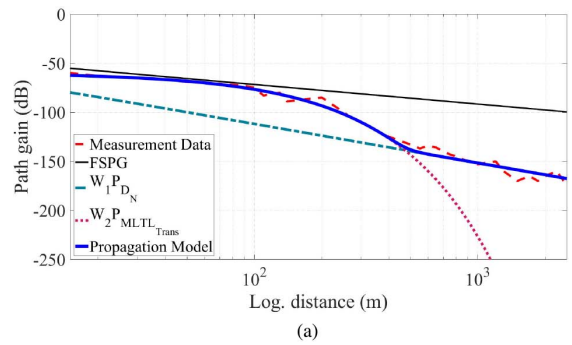
1) PROPAGATION MODEL

The transmission line, in parallel and uncoupled with the diffraction path, is depicted in Fig. 1. By considering trees as absorbing baffles with equal heights, and spacing *r*, (see Fig. 6), the multiple knife-edge attenuation, A_N, becomes frequency independent and simplifies to an exact solution given in [4]; i.e.,

$$A_N = \frac{1}{N+1}, \qquad (16)$$

where $N = d_T/r$ is the number of baffles between the transmitter and receiver. So for $r = 1$m, for example, and $d_T = 2580$m, we get $N = 2850$ (see caption of Fig. 7 for other choices of *r*), and the offset (Fig. 7a) is -68dB. The diffracted power is calculated from

$$P_{D_N} = G_{path}^{(FS)} \cdot (A_N)^2. \qquad (17)$$

In summary, the received power through the transmission line is $P_{MLTL_{Trans}} = \dfrac{|E_0|^2 |T|^2}{2\eta_0}$, using a frequency of 917.5MHz and an *M*-layer transmission line (*N* trees $= M/2$) with spacing *r* and the tree thickness $d = r/4$. These choices are almost arbitrary because the thickness, spacing and the value of the lossy permittivity can be interchanged for the same effect. The real part of the relative permittivity is taken
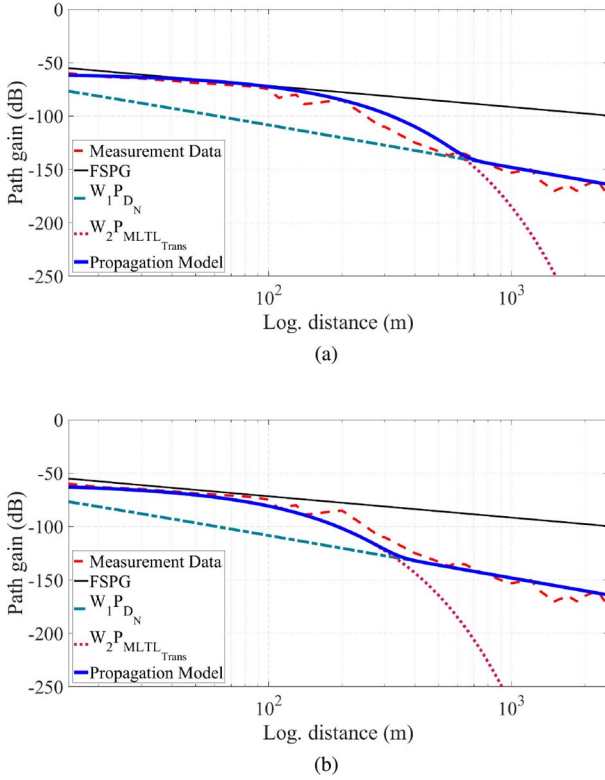

FIGURE 7. Comparison between the measured path gain in [23] and our propagation model for $\epsilon'' = 0.008$, $W_2 = 1 - W_1 = -70$dB: **(a)** $r = 1$m ($N = 2580$), **(b)** $r = 1.5$m ($N = 1720$), **(c)** $r = 2$m ($N = 1290$) and **(d)** $r = 3$m ($N = 860$). Note that for different *r*, *N* is different, and the distance scale is logarithmic. The free space path gain (FSPG), $W_1 P_{D_N}$, and $W_2 P_{MLTL_{Trans}}$ are also plotted to show the dominant parameters.

as one (i.e., same as free space), because only the loss behaviour is of interest, rather than the scattering detail.

The total received power is just
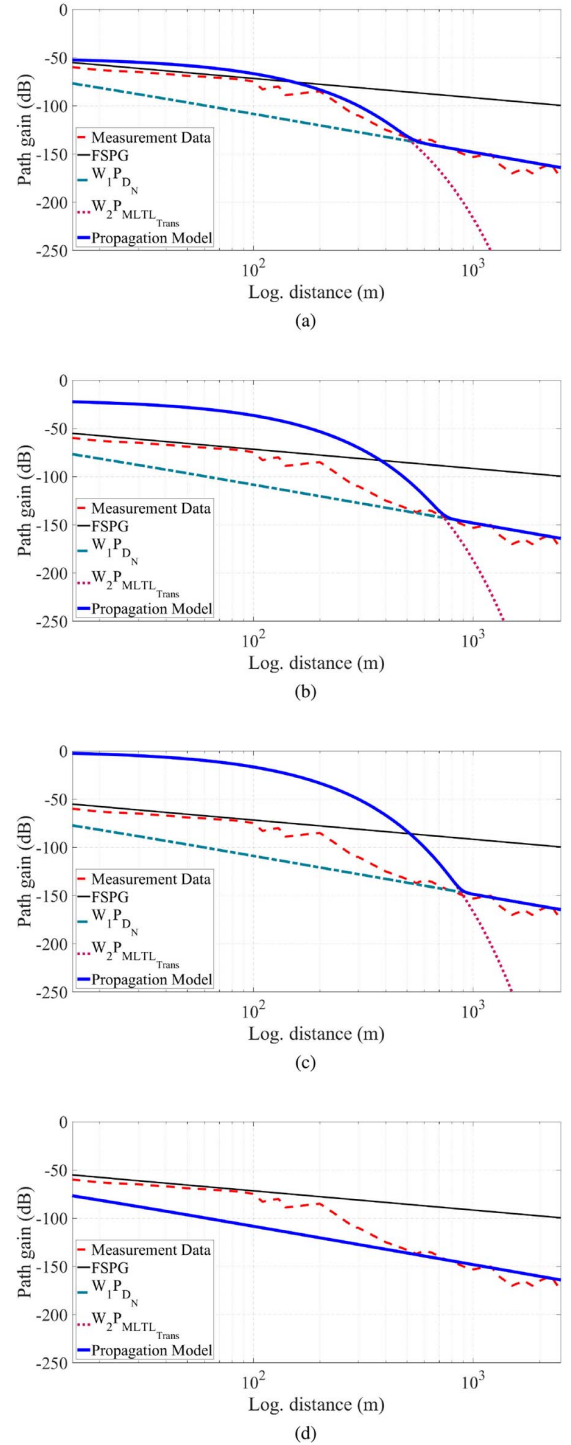
$$P_{R_{total}} = W_1 P_{D_N} + W_2 P_{MLTL_{Trans}}. \qquad (18)$$

FIGURE 8. Comparison between the measured path gain in [23] and our propagation model for $r = 1.5$m ($N = 1720$), $W_2 = 1 - W_1 = -70$dB: (a) $\epsilon'' = 0.006$ and (b) $\epsilon'' = 0.01$. The distance scale is logarithmic. The free space path gain (FSPG), $W_1 P_{D_N}$, and $W_2 P_{MLTL_{Trans}}$ are also plotted to show the dominant parameters.

2) EMPIRICAL PARAMETERS

The propagation model includes three empirical parameters; i.e., r, ϵ'' and W_1, found by fitting the experimental data. This section illustrates, using figures, the effect of these parameters on the dual-slope behaviour, with a simple numerical study. The figures below for the path gain have a large dynamic range in order to emphasize the macro-behaviour. The detail, within the dynamic range, is covered by evaluating the uncertainty in the form of a dB Root Mean Square Error (RMSE).

First, the effect of the spacing r is shown in Fig. 7 for $r = 1$, 1.5, 2 and 3m. The other parameters are fixed to $\epsilon'' = 0.008$ and $W_1 = 0.9999999$ (so the transmission line contribution offset is $W_2 = 1 - W_1 = -70$dB). The results indicate that the long-distance slope of the model which follows the diffracted power from around 500m to 2580m depends on the spacing r. (We could alternatively fix r and change ϵ'', etc, see below.) For $r = 1$m, the model fits the measurement nicely, giving the N.

The effect of ϵ'', is plotted in Fig. 8 for $\epsilon'' = 0.006$ and 0.01. The other parameters are fixed to $r = 1.5$m ($N = 1720$) and $W_2 = 1 - W_1 = -70$dB. The short-distance slope of the model, from 15 to around 200m, as well as the transition between two slopes from 200 to 500m change, are shown in the figure. In particular, it indicates how, in this model, changing ϵ'', while the trees' thickness-to-spacing ratio is fixed, or vice versa, affects the short-distance slope.

FIGURE 9. Comparison between the measured path gain in [23] and our propagation model for $\epsilon'' = 0.008$, $r = 1.5$m ($N = 1720$): (a) $W_2 = 1 - W_1 = -60$dB, (b) $W_2 = 1 - W_1 = -30$dB, (c) $W_2 = 1 - W_1 = -1$dB, (d) $W_2 = 1 - W_1 = -\infty$dB. The distance scale is logarithmic. The free space path gain (FSPG), $W_1 P_{D_N}$, and $W_2 P_{MLTL_{Trans}}$ are also plotted to show the dominant parameters.

Finally, Fig. 9 illustrates the weighting W_1 changing from 0.9 to 1 (i.e., W_2 changes from -1dB to $-\infty$dB) with $r = 1.5$m and $\epsilon'' = 0.008$. It shows how the diffraction is the more dominant mechanism for the long distance. But if only the diffraction mechanism is considered (i.e., when $W_1 = 1$), then the measured data from 15 to 500 meters

TABLE 1. RMS error of our propagation model with various empirical parameters.

Fig.	r(m)	$N = M/2$	ϵ''	$W_2 = 1 - W_1$(dB)	RMSE (dB)
7a	1	2580	0.008	-70	4.6
7b	1.5	1720	0.008	-70	4.9
7c	2	1290	0.008	-70	5.8
7d	3	860	0.008	-70	7.5
8a	1.5	1720	0.006	-70	6.9
8b	1.5	1720	0.01	-70	6.8
9a	1.5	1720	0.008	-60	8.3
9b	1.5	1720	0.008	-30	29.8
9c	1.5	1720	0.008	-1	45.6
9d	1.5	1720	0.008	$-\infty$	20.3

TABLE 2. RMS error of propagation model for vegetation.

Model	RMSE (dB)
The propagation model in Fig. 7a	4.6
Tewari* [39] for all measured data	10.2 [23]
Tewari* [39] from 200m	6.7 [23]
Two–Ray+2×ITU-R P.2108-0 [23] from 200m (Same height Tx and Rx)	7.6
ITU-R P.1546+2×ITU-R P.2108-0 [23] from 200m (Same height Tx and Rx)	11.2
RET model	13
Polynomial regression (n=1)	18.5
Polynomial regression (n=2)	7.9
Polynomial regression (n=3)	4.5
Polynomial regression (n=4)	4.33
Polynomial regression (n=5)	4.1
Polynomial regression (n=6)	3.5

cannot be fitted. By choosing a best value for W_1, the first slope from 15 to around 200 meters, as well as the transition between the two slopes between 200 and 500 meters, can also be fitted to the experimental data.

B. MODEL PERFORMANCE

RMSE in dB is calculated between the measured and predicted path gain (reciprocal of the path loss, or rather negative in dB, as used in the equation below [38]),

$$RMSE = \sqrt{\frac{\sum_{i=1}^{n}\left(G_{path_{m_i}}^{(dB)} - G_{path_{p_i}}^{(dB)}\right)^2}{n}} \quad [dB], \quad (19)$$

where n is the total number of measurements. The RMSE using the various empirical parameters of r, ϵ'' and W_1 are tabulated in Table 1.

The *RMSE* of the best fit to the experiments of [23] is 4.6 which is shown in Fig. 7a for $\epsilon'' = 0.008$, $r = 1$m and $W_2 = 1 - W_1 = -70$dB. This model is compared here using the RMSE of the following models. The results are summarized in Table 2.

The first model for comparison is a three-parameter (for a fixed frequency) empirical model proposed by Tewari *et al.* [39], where the path gain in dB is given by

$$G_{path} = -PL_{Tewari} = 27.57 - 20\log_{10}(f)$$
$$+ 20\log_{10}\left(\frac{Ae^{-\alpha_2 dist}}{dist} + \frac{B}{dist^2}\right) \quad [dB], \quad (20)$$

where f is the frequency in MHz, *dis* is the propagation distance in meters. A and B are constants found empirically, and α_2 is the constant describing the rate of the attenuation in dB/m [39]. This model is claimed to be been verified [39] for discrete frequencies between 50 to 800MHz. For comparison with the measured data at 917.5MHz, the empirical values for 800MHz have been used [23]. The RMSE of the Tewari model with the measured data for the total distance, as well as for the diffraction-dominated distances from 200m to 2580m, are given in Table 2.

The RMSE of the two models presented in [23] for distance from 200m to 2580m, are also included in Table 2.

Finally, the measured data is modeled using linear polynomial regression function, i.e., purely as a curve fit, with no reference to propagation mechanisms, given by

$$y = \beta_0 + \beta_1 x + \beta_2 x^2 + \beta_3 x^3 + \cdots + \beta_n x^n \quad (21)$$

for $n \in \{1, 2, 3, 4, 5, 6\}$. The results are also in Table 2.

Our two-mechanism model, with three empirical parameters for a fixed frequency, has a smaller uncertainty (RMSE = 4.6) compared to the other models and its uncertainty is close to the 3rd degree polynomial function. Compared to the various models treated in [23], our model gives a better fit for the distance from 15m to the furthest point at over 2580m, whereas the model in [23] is from 200m. The four-parameter RET model (proposed for only short distances), for a fixed frequency, has RMSE = 13dB. We have not included an explicit frequency dependence for our model, however the free space component in the diffraction contribution, and the transmission line equations, contain the frequency dependence. Without similar, long-distance measurements being available at other frequencies, we cannot verify a frequency dependence for this model. We note that [40] gives some measurements well spread around 1GHz for long distances, but these are over undulating terrain using a vehicular antenna (the measurements we use are truly through-forest with a personal antenna system) where other mechanisms, such as terrain-shadowing, are at play.

IV. SUMMARY AND CONCLUSION

Propagation through a forest features dual-slope behaviour in the log-log path gain. For NLOS short distances (less than a couple of hundred meters), there is a free-space-like slope with a large offset of about -60dB; and for long distances (more than about five hundred meters), there is a steeper slope with another offset. This dual-slope behaviour suggests two principal propagation mechanisms. For the short-distance, it is intuitive that there is direct transmission through the foliage. This can be modeled by the RET, but the simplest model for this is a linear, low-attenuation transmission line where a succession of lossy sections are separated by lossless sections. There is an interchangeable choice of parameters for configuring such a transmission line model, but the loss is only from the lossy sections instead of also from spherical or cylindrical spreading. This transmission line behaviour is shown here to be able to match the experimental short-distance propagation. It has the advantage over the standard short-distance RET model of being simpler and having fewer fitting parameters. This transmission line (or the RET model, etc) cannot also provide

a match for the long-distance propagation, nor the transition region between the dual slopes. This is because even a linear transmission line gain falls away very quickly with longer distance, which is contrary to the experimental facts. The simplest and most reasonable physical mechanism is a parallel transmission path over the tree tops. A model for this is multiple knife-edge diffraction, where the trees are the knife-edges, and this further reduced by modeling the tree tops as being constant height and spacing. This model is therefore extremely simple, has minimal parameters, and yet retains a reasonable attachment to the physics. We demonstrate that such a diffraction wave can match the long-distance slope of through-forest propagation. We also demonstrate that a weighted combination (i.e., parallel paths) of the two modeled mechanisms accurately matches (RMSE as low as 5dB) the whole range of the experimental measurement - the dual slopes, their offsets, and the transition region between the short- and long-distances.

REFERENCES

[1] R. Luebbers, "Finite conductivity uniform GTD versus knife edge diffraction in prediction of propagation path loss," *IEEE Trans. Antennas Propag.*, vol. AP-32, no. 1, pp. 70–76, Jan. 1984.

[2] R. G. Kouyoumjian and P. H. Pathak, "A uniform geometrical theory of diffraction for an edge in a perfectly conducting surface," *Proc. IEEE*, vol. 62, no. 11, pp. 1448–1461, Nov. 1974.

[3] D. A. McNamara, C. Pistorius, and J. Malherbe, *Introduction to the Uniform Geometrical Theory of Diffraction*. Norwood, MA, USA: Artech, 1990.

[4] S. W. Lee, "Path integrals for solving some electromagnetic edge diffraction problems," *J. Math. Phys.*, vol. 19, no. 6, pp. 1414–1422, Jun. 1978.

[5] L. E. Vogler, "The attenuation of electromagnetic waves by multiple knife-edge diffraction," Natl. Telecommun. Inf. Admin., Boulder, CO, USA, Rep. 81-86, p. 20, Oct. 1981.

[6] L. E. Vogler, "An attenuation function for multiple knife-edge diffraction," *Radio Sci.*, vol. 17, no. 6, pp. 1541–1546, Nov. 1982.

[7] J. B. Andersen, "UTD multiple-edge transition zone diffraction," *IEEE Trans. Antennas Propag.*, vol. 45, no. 7, pp. 1093–1097, Jul. 1997.

[8] R. G. Vaughan and J. Andersen, *Channels, Propagations and Antennas for Mobile Communications*, 1st ed., London, U.K.: Inst. Elect. Eng., 2003.

[9] C. Tzaras and S. R. Saunders, "An improved heuristic UTD solution for multiple-edge transition zone diffraction," *IEEE Trans. Antennas Propag.*, vol. 49, no. 12, pp. 1678–1682, Dec. 2001.

[10] C. Tzaras and S. R. Saunders, "Rapid, uniform computation of multiple knife-edge diffraction," *Electron. Lett.*, vol. 35, no. 3, pp. 237–239, Feb. 1999.

[11] R. Zabihi and R. G. Vaughan, "Comparison of diffraction with numerical and physical experiments," in *Proc. IEEE Int. Symp. Antennas Propag. Nat. Radio Sci. Meeting (USNC/URSI)*, Jul. 2015, pp. 1796–1797.

[12] R. Zabihi and R. G. Vaughan, "Diffraction: A critical propagation mechanism," in *Proc. IEEE Can. Conf. Elect. Comput. Eng. (CCECE)*, May 2016, pp. 1–4.

[13] T. Negishi *et al.*, "Measurements to validate the UTD triple diffraction coefficient," *IEEE Trans. Antennas Propag.*, vol. 62, no. 7, pp. 3723–3730, Jul. 2014.

[14] M. D. Estarki and R. G. Vaughan, "Software-based design of multiple antenna systems for large wireless capacities," in *Proc. Meetings Wireless World Res. Forum (WWRF)*, Oct. 2013, pp. 751–756.

[15] M. D. Estarki, C. Hynes, A. Lea, and R. G. Vaughan, "A review of the radio wave propagation through vegetation," in *Proc. IEEE Int. Symp. Antennas Propag. Nat. Radio Sci. Meeting (USNC/URSI)*, Jul. 2017, pp. 801–802.

[16] M. O. Al-Nuaimi and R. B. L. Stephens, "Measurements and prediction model optimisation for signal attenuation in vegetation media at centimetre wave frequencies," *IEE Proc. Microw. Antennas Propag.*, vol. 145, no. 3, pp. 201–206, Jun. 1998.

[17] M. P. M. Hall, "Cost project 235 activities on radiowave propagation effects on next-generation fixed-service terrestrial telecommunication systems," in *Proc. 8th Int. Conf. Antennas Propag.*, vol. 2, Mar. 1993, pp. 655–659.

[18] "Attenuation in vegetation," Int. Telecommun. Union, Geneva, Switzerland, ITU-Recommendation 833-9, 2016.

[19] M. A. Weissberger, "An initial critical summary of models for predicting the attenuation of radio waves by trees," IIT Res. Inst., Electromagn. Compatibility Anal. Center, Annapolis, MD, USA, Rep. FSD-TR-81-101, Jul. 1982.

[20] Y. S. Meng, Y. H. Lee, and B. C. Ng, "Empirical near ground path loss modeling in a forest at VHF and UHF bands," *IEEE Trans. Antennas Propag.*, vol. 57, no. 5, pp. 1461–1468, May 2009.

[21] G. Durgin, T. S. Rappaport, and H. Xu, "Measurements and models for radio path loss and penetration loss in and around homes and trees at 5.85 GHz," *IEEE Trans. Commun.*, vol. 46, no. 11, pp. 1484–1496, Nov. 1998.

[22] Z. I. Rizman, K. Jusoff, S. S. Rais, H. H. A. Bakar, G. K. S. Nair, and Y. K. Ho, "Microwave signal propagation on oil palm trees: Measurements and analysis," *Int. J. Smart Sens. Intell. Syst.*, vol. 4, no. 3, pp. 388–401, 2011.

[23] J. Hejselbæk, J. Ø. Nielsen, W. Fan, and G. F. Pedersen, "Empirical study of near ground propagation in forest terrain for Internet-of-Things type device-to-device communication," *IEEE Access*, vol. 6, pp. 54052–54063, 2018.

[24] Y. Zhang, C. R. Anderson, N. Michelusi, D. J. Love, K. R. Baker, and J. V. Krogmeier, "Propagation modeling through foliage in a coniferous forest at 28 GHz," *IEEE Wireless Commun. Lett.*, vol. 8, no. 3, pp. 901–904, Jun. 2019.

[25] A. Ishimaru, *Wave Propagation and Scattering in Random Media*. New York, NY, USA: Academic, 1978.

[26] K. Sarabandi and I.-S. Koh, "A complete physics-based channel parameter simulation for wave propagation in a forest environment," *IEEE Trans. Antennas Propag.*, vol. 49, no. 2, pp. 260–271, Feb. 2001.

[27] F. Wang and K. Sarabandi, "An enhanced millimeter-wave foliage propagation model," *IEEE Trans. Antennas Propag.*, vol. 53, no. 7, pp. 2138–2145, Jul. 2005.

[28] F. Wang and K. Sarabandi, "A physics-based statistical model for wave propagation through foliage," *IEEE Trans. Antennas Propag.*, vol. 55, no. 3, pp. 958–968, Mar. 2007.

[29] R. Johnson and F. Schwering, "A transport theory of millimeter wave propagation in woods and forest," U.S. Army CECOM FORT, Monmouth, NJ, USA, Rep. CECOM-TR-85-1, Feb. 1985.

[30] F. K. Schwering, E. J. Violette, and R. H. Espeland, "Millimeter-wave propagation in vegetation: Experiments and theory," *IEEE Trans. Geosci. Remote Sens.*, vol. 26, no. 3, pp. 355–367, May 1988.

[31] N. Rogers *et al.*, "A generic model of 1–60 GHz radio propagation through vegetation," Radiocommun. Agency, U.K., Rep. QINETIQ/KI/COM/CR020196/1.0, May 2002.

[32] D. L. Ndzi *et al.*, "Vegetation attenuation measurements and modeling in plantations for wireless sensor network planning," *Progr. Electromagn. Res.*, vol. 36, pp. 283–301, Jan. 2012.

[33] R. Zabihi and R. G. Vaughan, "Simple transmission line model from RET results for propagation through vegetation," in *Proc. IEEE Int. Symp. Antennas Propag. Nat. Radio Sci. Meeting (USNC/URSI)*, Boston, MA, USA, Jul. 2018, pp. 1329–1330.

[34] J. R. Wait, *Electromagnetic Wave Theory*. New York, NY, USA: Harper and Row, 1985.

[35] S. J. Orfanidis, *Electromagnetic Waves and Antennas*, Rutgers Univ., New Brunswick, NJ, USA, 2002. [Online]. Available: https://www.ece.rutgers.edu/orfanidi/ewa/

[36] K. Furutsu, "On the theory of radio wave propagation over inhomogeneous earth," *J. Res. Nat. Bureau Stand. D. Radio Propag.*, vol. 67-D, no. 1, pp. 39–62, Feb. 1963.

[37] K. Rizk, R. Valenzuela, D. Chizhik, and F. Gardiol, "Application of the slope diffraction method for urban microwave propagation prediction," in *Proc. 48th IEEE Veh. Technol. Conf. (VTC)*, vol. 2, May 1998, pp. 1150–1155.

[38] J. Wu and D. Yuan, "Propagation measurements and modeling in Jinan city," in *Proc. 9th IEEE Int. Symp. Pers. Indoor Mobile Radio Commun.*, vol. 3, Sep. 1998, pp. 1157–1160.

[39] R. Tewari, S. Swarup, and M. Roy, "An empirical result for the height gain in forest medium," *IEEE Trans. Antennas Propag.*, vol. AP-32, no. 11, pp. 1265–1268, Nov. 1984.

[40] I. Z. Kovacs, P. C. F. Eggers, and K. Olesen, "Radio channel characterisation for forest environments in the VHF and UHF frequency bands," in *Proc. IEEE VTS 50th Veh. Technol. Conf. 21st Century Commun. Village (VTC-Fall)*, vol. 3, Sep. 1999, pp. 1387–1391.